



Short communication

Electrochemical investigation of an artificial solid electrolyte interface for improving the cycle-ability of lithium ion batteries using an atomic layer deposition on a graphite electrode

Hsin-Yi Wang^a, Fu-Ming Wang^{a,b,*}

^aSustainable Energy Center, National Taiwan University of Science and Technology, Taipei, Taiwan

^bGraduate Institute of Applied Science and Technology, National Taiwan University of Science and Technology, Taipei, Taiwan

HIGHLIGHTS

- The artificial SEI layer is fabricated by atomic layer deposition (ALD).
- The artificial SEI is used to prevent the decomposition at high temperature of the electrolytes.
- The battery that used the ALD-TiO₂-coated graphite showed excellent cycle retention at 55 °C.

ARTICLE INFO

Article history:

Received 16 August 2012

Received in revised form

27 December 2012

Accepted 19 January 2013

Available online 28 January 2013

Keywords:

ALD

SEI

Lithium ion battery

Graphite

High temperature

ABSTRACT

Electrochemically formed solid electrolyte interfaces (SEIs) are the crucial link between electrolytes and electrodes because they enable several functions in lithium ion batteries, including ionic diffusion, electric conduction, and the safety provided by thermal stability. However, fabricating the electrochemical formed in SEI entails accuracy regarding its architecture to create the specific electrolyte composition that is mutually compatible with the electrode materials. This process, however, is difficult and hinders the industrial application and development of lithium ion batteries. In this study, the atomic layer deposition (ALD) technique is used in artificial SEI fabrication to deposit a metal oxide on the graphite anode's surface. In addition, the effects of the artificial SEI-applied Al₂O₃ and TiO₂ on the charge–discharge performance and cycling behavior at 55 °C were investigated. Electrochemical performance was analyzed by an impedance and cyclic voltammogram to show that an ALD coating of TiO₂ provides crucial functions for graphite. The results indicated that the TiO₂ coating increased the graphite capacity by 5% and limited the formation of electrochemically formed SEIs. In addition, the TiO₂-coating graphite with ALD improved thermal stability and greatly enhanced long-term cycle ability at 55 °C.

© 2013 Elsevier B.V. All rights reserved.

1. Introduction

High energy density of Li batteries makes them useful in hybrid electric and plug-in electric vehicles (HEVs and PHEVs), which have been proposed as the next modes of transportation. However, several rigorous criteria for Li batteries must be considered, including stable operations at a wide temperature range (−30–60 °C), a long cycle life, high tolerances under various charge/discharge rates, and the possession of high energy density [1]. Based on thermodynamic theory, the lowest unoccupied molecular orbital (LUMO)

of a non-aqueous solvent and electrolyte additive should be higher than the graphite because of the higher reduction potential of electrolytes, causing solid electrolyte interface (SEI) formation during the first cycle [2]. Although a well-functionalized SEI reinforces the electrochemical stability of the graphite anode [3], SEIs decompose easily at high temperatures because of hydrofluoric acid (HF) formation, which decomposes lithium salt and has various influences on SEI. These reactions initiate a thermo-runaway reaction, triggering the explosion of the battery.

Previous studies have investigated various methods to prevent SEI decomposition at high temperatures, such as graphite surface modification with metal/metal oxide deposition or polymer coating, surface mild oxidation, and un-carbon-based anodes [4]. However, some of the surface modifications, such as the sol–gel method [5,6], require high-temperature processes and large

* Corresponding author. IB 606, 43 Keelung Road, Section 4, Taipei 106, Taiwan.
Tel.: +886 2 27303755; fax: +886 2 27376922.

E-mail address: mccabe@mail.ntust.edu.tw (F.-M. Wang).

quantities of solvent. In addition, the electric conduction pathway between the active and the coating materials should be well established to reinforce the electron transfer during the redox reaction. However, electric conductivity is restricted by sophisticated coating methods because the thickness and uniformity of the coating materials cannot be precisely controlled.

Atomic layer deposition (ALD) is an advanced technology for applying ultrathin and homogenous films on high-surface specimens using a self-limited reaction at below 100 °C [7]. Jung et al. reported an ALD method to apply a thin layer of Al₂O₃ coating on natural graphite, demonstrating an improvement in cycle-ability [8]. However, Al₂O₃ is not an ideal material for Li batteries because it does not provide intercalation and extraction functions. Therefore, Al₂O₃ can only be used as a stabilizer to solidify the graphite structure and to prevent superfluous electrochemical reactions. Consequently, TiO₂ is a potential anode material because it possesses an appropriate crystal structure for serving as the host electrode for Li ions. In addition, TiO₂-coated anodes or cathodes have impressive electrochemical performances because of their high electric conductivity [8–11].

In this study, ALD-TiO₂-coated graphite was used to comprehensively compare bare and ALD-Al₂O₃-coated graphite to discuss their effects on electric conductivity and the host performance. Furthermore, 55 °C was selected as the testing temperature of cycle-ability at which to appraise the vehicular application.

2. Experimental

The lithium ion batteries used in this study were disassembled from type 503709C cells provided by EXA CO. in Taiwan (ALB, aluminum-plastic laminated film exterior with dimensions of 5.0 × 37 × 59 mm). The graphite anode was composed of meso-carbon microbeads (93 wt%; MCMB-2528, Osaka Gas), PVDF, which was the binder (4 wt%), and Ks-6, which was the conductive additive (3 wt%) to fabricate a composite anode electrode. The composite anode electrode was directly placed into the reaction chamber and waited for the ALD process. The precursors used for the Al₂O₃/TiO₂ ALD were water, trimethylaluminum [(TMA), Al(CH₃)₃], and Titanium tetrabromide, TiBr₄. A low reaction temperature was used because PVDF requires a low processing temperature (m.p. < 150 °C). The Al₂O₃/TiO₂ ALD reaction cycle consisted of the following steps that were performed on a H₂O-prepulsed (10.0 Torr for 4 s with 10 cycles) electrode: 1) The introduction of sufficient TMA or TiBr₄ to increase the pressure to 10.0 Torr for 4 s; 2) the evacuation of the reaction products and excess TMA or TiBr₄ to control the pressure at 0.5 Torr for 12 s; 3) the introduction of H₂O to increase the pressure to 10.0 Torr for 4 s; and 4) the evacuation of the reaction products and excess H₂O to achieve a pressure of 0.5 Torr for 12 s. The TEM image in previous studies shown that the thickness of the thin Al₂O₃/TiO₂ film following 100 ALD cycles was 20–30 nm [7]. The crystal structure of Al₂O₃/TiO₂ film on graphite surface has been identified as well as the previous studies [12,13].

In the coin cells, separators (Celgard 2320) were placed between the graphite as working and lithium metal as the counter electrodes. The electrolyte was 1.0 M LiPF₆ (Tomiyama Pure Chemical, Japan) in an ethylene carbonate (EC)/propylene carbonate (PC)/diethyl carbonate (DEC) mixed solvent at a 3:2:5 volume ratio, respectively. Electrochemical tests were conducted by a Bio-logic potentiostat (VMP3) at 25 °C. The diffusion coefficients were obtained through cyclic voltammetry (CV) scanning rates at 0.5, 1.0, 3, and 5 mV s⁻¹. According to the Randles–Sevcik equation (shown below), the magnitude of the peak current (I_p) is a function of the temperature ($T = 298.15$ K), lithium ion concentration ($C_{LiPF_6} = 1.0$ M), electrode area ($A = 1.33$ cm²), number of electrons transferred ($n = 1$), diffusion coefficient (D), and scanning rate (ν).

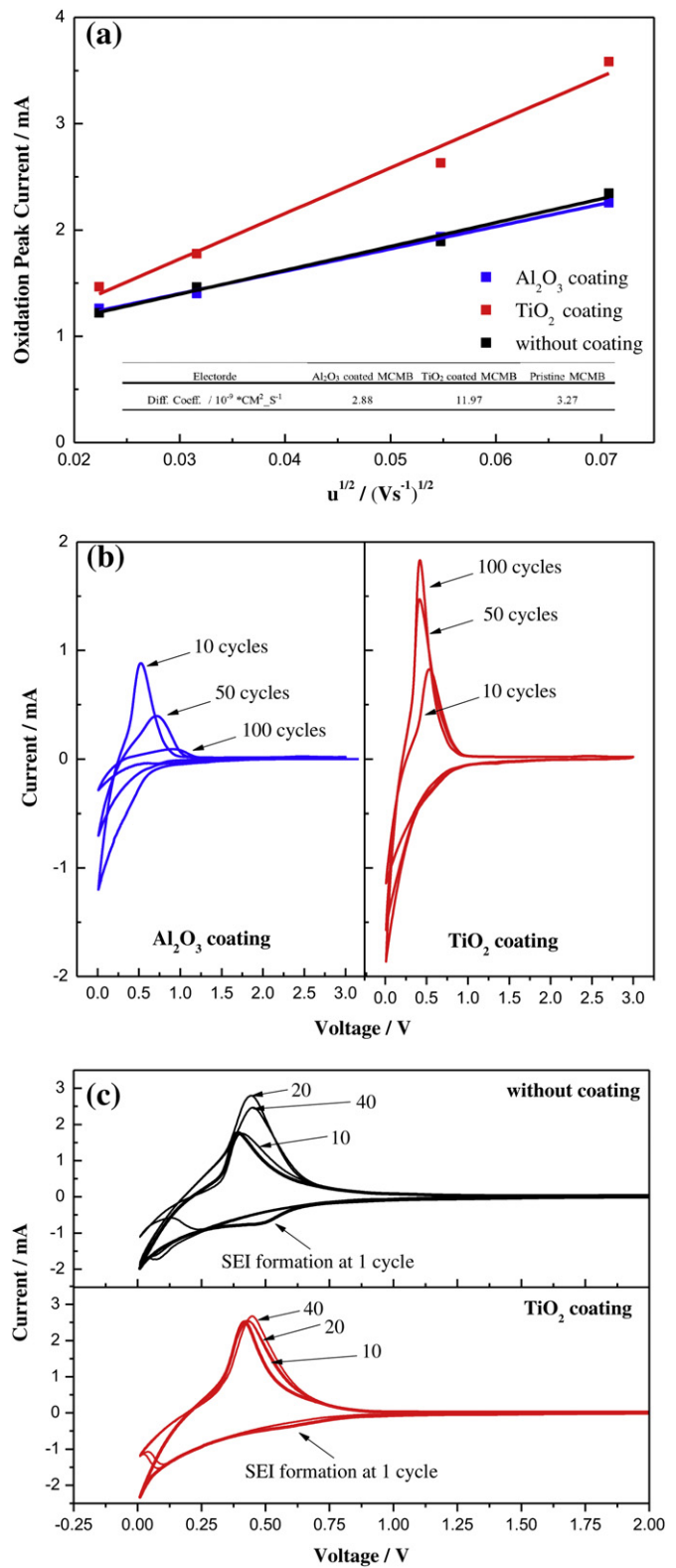


Fig. 1. (a) The Randles–Sevcik plot with various scanning rates at 0.5, 1, 3 and 5 mV s⁻¹ during Li extraction process, (b) cyclic voltammetry of ALD Al₂O₃ coated MCMB and ALD TiO₂ coated MCMB with various thickness of 10, 50 and 100 cycles of ALD reaction, (c) cyclic voltammetry of MCMB and ALD TiO₂ coated MCMB with various scan at the 1, 10, 20 and 40 times on 0.5 mV s⁻¹.

$$I_p = 0.4463nFA \left(\frac{nF}{RT} \right)^{1/2} D^{1/2} v^{1/2} C_{\text{LiPF}_6}$$

Electrochemical impedance spectroscopy (EIS) was examined in the frequency range of 10 MHz to 0.01 Hz with an AC amplitude of 5 mV. To examine the cycling performance, the cells were cycled 3 times with a constant current of 0.2 C between 3.0 V and 0.01 V at 25 °C for the initial SEI formation. These cells were further charged and discharged at 0.2 C for 40 cycles at 55 °C using a UBQ battery charger (series CHG-5500C).

3. Results

3.1. Cyclic voltammogram

Fig. 1a shows a Randles–Sevcik plot that indicates the ionic diffuse kinetic behaviors of various electrodes with different scanning rates. The plating diffusion coefficient of the 10 cycle layers of ALD-Al₂O₃-coated graphite ($2.88 \times 10^{-9} \text{ cm}^2 \text{ s}^{-1}$) was slightly less than that of the bare graphite ($3.27 \times 10^{-9} \text{ cm}^2 \text{ s}^{-1}$), demonstrating that the ALD Al₂O₃-coated layer plays a crucial role in slowing the electron transfer and limiting the ionic transfer to the electrode surface. In contrast to the 10 cycle layers of ALD-TiO₂-coated graphite, the ALD-TiO₂-coated graphite had a diffusion coefficient that was more than 4 times faster ($11.97 \times 10^{-9} \text{ cm}^2 \text{ s}^{-1}$) than the other two electrodes. To further elucidate the substantial increment between Al₂O₃ and TiO₂, two ALD-coated graphites were used to estimate the effects of various thicknesses and to examine the electrochemical behavior of Al₂O₃ and TiO₂ with CV.

Fig. 1b shows that the redox peak current (I_p) of the ALD-TiO₂-coated graphite became higher in accordance to the increasing coating thickness. However, the ALD-Al₂O₃-coated graphite had the opposite reaction, and decreased when the thickness increased. In addition, the plating and stripping potentials of the lithium ions in the ALD-TiO₂-coated graphite showed a slightly identical increase in accordance to the increased thickness. However, the plating and

stripping potentials of the lithium ions in the ALD-Al₂O₃-coated graphite immediately shifted to the late potential. According to these results, the redox behaviors indicated that the electrochemical reactions occurred precisely on the electrode/electrolyte interface. Fast mass transport supplements of the ionic diffusion can benefit this reaction, resulting in a larger peak current on the CV plot. Because Al₂O₃ is not a perfect electron conductor and is an electrochemically inactive material, an over-coated Al₂O₃ hinders ionic channels, creating a kinetic bottleneck. Therefore, electrons move slowly through the ALD-Al₂O₃-coated graphite, and there is a perceptible time lag between the potential at the voltage source and at the electrode/electrolyte interface, rather than enhancing the graphite structural stability. However, the ALD-TiO₂-coated graphite showed different results because the nanostructure of TiO₂ provides higher electron affinity (E.A.) than Al₂O₃ [11,14,15] and builds up a well contact [16] between the electrolyte and the electrode surfaces, facilitating the passing of lithium ions through the interface. In addition, TiO₂ is an ideal host material for lithium ion batteries [17] and has become a preferred electrochemical reactant.

Additional benefits of TiO₂ include a voltage plateau of 1.2–1.5 V, meaning that almost no electrochemically formed SEI can be produced on this material. **Fig. 1c** shows the CV measurements of the 10 cycle layers of ALD-TiO₂-coated graphite and a comparison with the bare graphite under increasing times of scan. Electrochemically formed SEI formed at the 0.4–0.6 V range during the first plating direction of the bare graphite. However, the ALD-TiO₂-coated graphite did not provide an obviously conventional SEI growing on this material. However, tiny amount of conventional SEI can be defined by the differential plot of **Fig. 1c** and this ALD-TiO₂-coated graphite is really covered with the artificial SEI (ALD TiO₂) first and tiny amount of conventional SEI later. Some literature also investigated the conventional SEI is formed on the TiO₂ [17,18]. Following 40 cycles, the ALD-TiO₂-coated graphite possessed a stable electrochemical behavior determined by its curve trace, integral area, and reaction potentials, which are nearly invariable. Dissimilar to

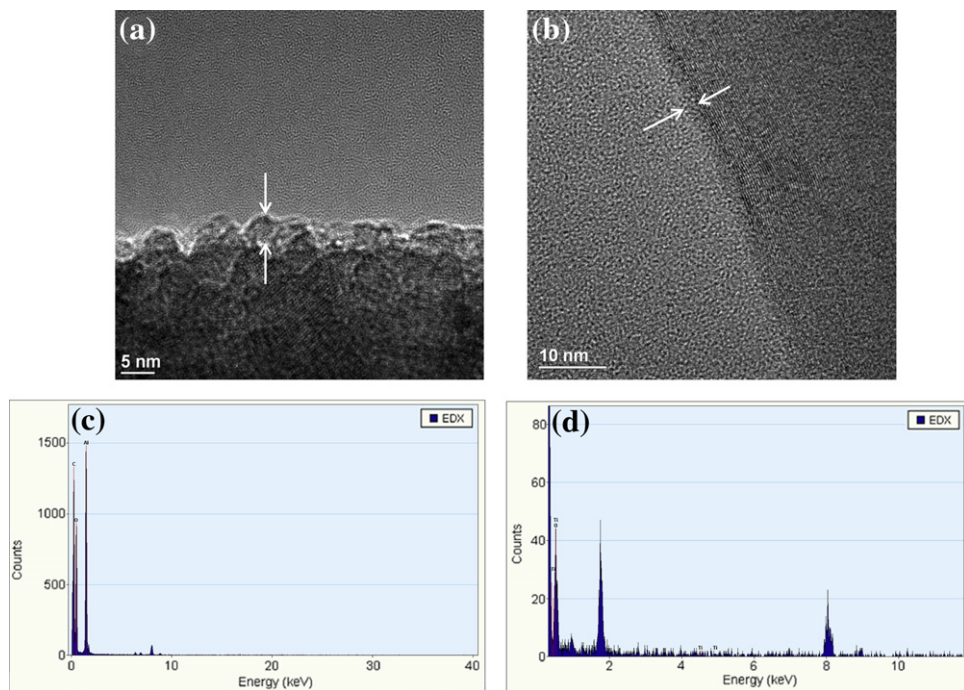


Fig. 2. The TEM microcopies of (a) ALD Al₂O₃ coated MCMB and (b) ALD TiO₂ coated MCMB with the thickness of 10 cycles of ALD reaction; the EDS analysis (the region between two arrows indication) of (c) ALD Al₂O₃ coated MCMB and (d) ALD TiO₂ coated MCMB with the thickness of 10 cycles of ALD reaction.

the ALD-TiO₂-coated graphite, the bare graphite changed its electrochemical behavior following 10 cycles, and polarization started because the electrochemical formed SEI restricted the ionic transport and electron transfer after battery was aged. Therefore, the ALD-TiO₂-coated layer, hereafter known as the “artificial SEI layer”, was used to prevent the decomposition of the solvents or electrolytes initiated by electrons tunneling through the SEI layer.

However, researchers believe that performance improvement is finite if the thickness of the TiO₂ coating layer is infinitely increased. The limiting influences of the thickness of the ALD-TiO₂-coating graphite are discussed below.

3.2. Morphology analysis

Fig. 2a and b shows the TEM microscopy of the ALD Al₂O₃ coated MCMB and the ALD TiO₂ coated MCMB with the thickness of 10 cycles of ALD reaction. According to the figures, the two white arrows clearly indicate an amorphous material formed and covered onto the high lattice crystal phase structure of LiCoO₂. These two figures demonstrate that the ALD Al₂O₃ and ALD TiO₂ coating provide 4–5 nm and 3 nm of thinness on MCMB, respectively. In addition, **Fig. 2a and b** also shows an excellent coating of metal oxide by using the ALD process, suggesting the ALD is employed on the composite electrode and the metal oxide is not deposited at contact points between active material particles and the current collector. This directly manufacturing process of ALD maintains electrical conductivity and enabling rapid electron transport of electrode [12]. **Fig. 2c and d** illustrates the EDS analysis of the regions that are indicated by the two white arrows in **Fig. 2a and b**. These regions show the aluminum and titanium formation, indicating the ALD coating onto the anode composite electrode is successful.

3.3. Cycle life and impedance analysis

Fig. 3a shows the discharging cycle life measurements of the half cells at 55 °C. Results revealed that the first cycle of the ALD-TiO₂-coated graphite possessed an enhanced capacity (344 mAh g⁻¹) compared to that of bare graphite (328 mAh g⁻¹), indicating that the ALD-TiO₂-coated layer can be used as a lithium ion host material. Following 40 cycles, the ALD-TiO₂-coated graphite maintained a high capacity about 300 mAh g⁻¹ at 55 °C. However, the bare graphite exhibited a fading capacity that became substantial following 20 cycles, indicating that electrochemically formed SEIs do not provide suitable protection under cycling at high temperatures. The improved cycle life of the ALD-TiO₂-coated layer prevented the decomposition of the graphite structures at 55 °C.

To investigate the surface properties of the 10 cycle layers of ALD-TiO₂-coated and bare graphites, impedance was measured to identify the resistance effects of the protection capability of the metal oxide layer. **Fig. 3b** shows an EIS Nyquist plot measured following 40 cycles at 55 °C. An equivalent circuit model demonstrating the internal construction of the battery is shown in **Fig. 3b**. The overall impedance included series resistance (R_s), which represented the external wire and electrolyte resistances; the first CPE₁- R_1 element, representing the impedance of the SEI layer; the second CPE₂- R_2 element, showing the impedance of interface between the SEI layer and the electrode material; the Warburg element (Z_w), which shows the diffusion resistance of the lithium ion in the electrode material; and the intercalation capacity (C_0) [19]. The fitting results are summarized and shown in the table located in **Fig. 3b**. Because all of the batteries used the same electrolyte, the two R_s were nearly identical. The R_1 value was strongly influenced by the surface morphology and the electrochemical properties of the SEI on the graphite. The ALD-TiO₂-coated graphite

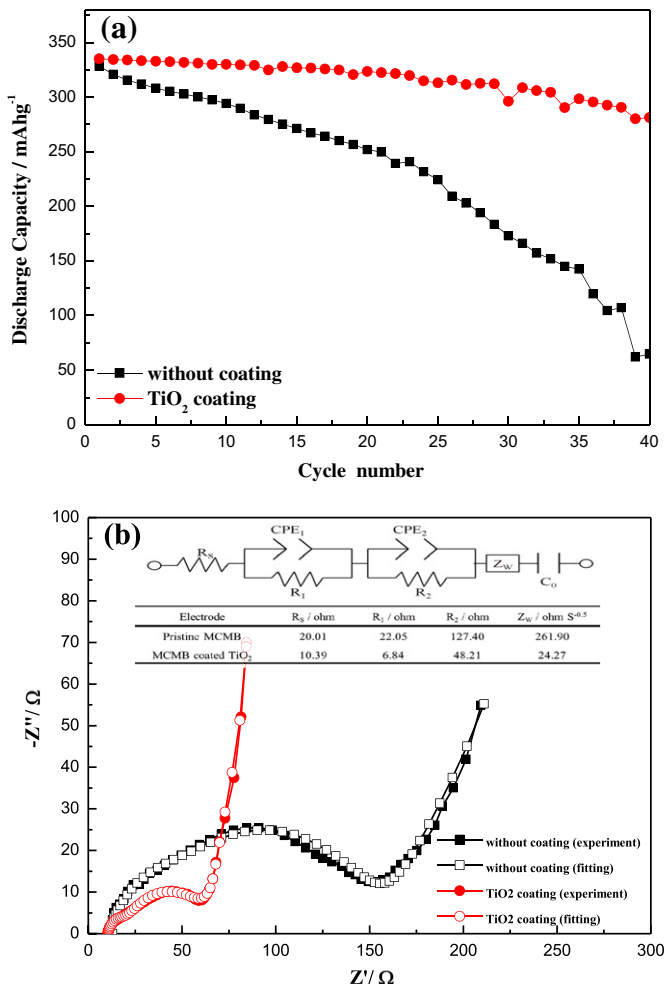


Fig. 3. (a) Cycle characteristics of the cells at 55 °C and (b) electrochemical impedance (solid)/simulating results (hollow spot) of the cells. The equivalent circuit model used to interpret the internal battery construction and the values of the parameters in the equivalent circuit from the simulation are shown in the Nyquist plot.

had a lower R_1 (6.84 Ω) compared to the bare graphite electrode (22.05 Ω), revealing that the bare graphite generated an electrochemically formed SEI that exhibited a high R_1 value during the same cycle, indicating that the high-temperature environment triggered the decomposition of SEIs, reducing ionic transfer. In contrast, the TiO₂ layer stabilized the surface property that provides lower activation energy because it had less SEI formation and facilitated ionic transfer. A good surface modification not only stabilizes the structure of the electrode, but also provides a suitable ionic channel for ionic intercalation. Furthermore, the ALD-TiO₂-coated graphite possessed a lower R_2 (48.21 Ω) value compared to the bare graphite (127.4 Ω), indicating that the TiO₂ structure made excellent contact with the ionic conductors, even after 40 cycles at 55 °C. The R_2 value of bare graphite revealed that high temperatures decompose electrochemically formed SEI, impeding lithium ion intercalation and further accelerating the capacity fading shown by the data in **Fig. 3a**.

4. Conclusion

This study examined the artificial SEI of an ALD-coated graphite and performed an electrochemical performance analysis. The battery that used the ALD-TiO₂-coated graphite showed excellent cycle

retention at 55 °C, and the discharge capacity was substantially enhanced. Compared to the electrochemically formed SEI, this method should be considered for application in future electric vehicles. Furthermore, these results suggest that coating thicknesses and materials affect ionic diffusion behaviors in various manners.

Acknowledgment

The authors are grateful for financial supporting this research from the National Science Council of Taiwan R.O.C under Grant NSC 100-2628-E-011-018-MY2, 100-2923-E-011-001-MY3, 102-3113-E-011-002 and 102-ET-E-011-003-ET.

References

- [1] S. Amjad, S. Neelakrishnan, R. Rudramoorthy, Renew. Sustain. Energy Rev. 14 (2010) 1104.
- [2] J.B. Goodenough, Y. Kim, Chem. Mater. 22 (2010) 587.
- [3] F.M. Wang, H.M. Cheng, H.C. Wu, S.Y. Chu, C.S. Cheng, C.R. Yang, Electrochim. Acta 54 (2009) 3344.
- [4] L.J. Fu, H. Liu, C. Li, Y.P. Wu, E. Rahm, R. Holze, H.Q. Wu, Solid State Sci. 8 (2006) 113.
- [5] S.W. Lee, K.S. Kim, H.S. Moon, H.J. Kim, B.W. Cho, W.I. Cho, J.B. Ju, J.W. Park, J. Power Sources 126 (2004) 150.
- [6] H.H. Chang, C.C. Chang, C.Y. Su, H.C. Wu, M.H. Yang, N.L. Wu, J. Power Sources 185 (2008) 466.
- [7] J.T. Lee, F.M. Wang, C.S. Cheng, C.C. Li, C.H. Lin, Electrochim. Acta 55 (2010) 4002.
- [8] Y.S. Jung, A.S. Cavanagh, L.A. Riley, S.H. Kang, A.C. Dillon, M.D. Groner, S.M. George, S.H. Lee, Adv. Mater. 22 (2010) 2172.
- [9] J.H. Lee, M.H. Hon, Y.W. Chung, I.C. Leu, Appl. Phys. A 102 (2011) 545.
- [10] Y. He, X. Yu, Y. Wang, H. Li, X. Huang, Adv. Mater. 23 (2011) 4938.
- [11] H.M. Cheng, F.M. Wang, J.P. Chu, R. Santhanam, J. Rick, S.C. Lo, J. Phys. Chem. C 116 (2012) 7629.
- [12] S.K. Chean, E. Perre, M. Rooth, M. Fondell, A. Harsta, L. Nyholm, M. Boman, T. Gustafsson, J. Li, P. Simon, K. Edstrom, Nano Lett. 9 (2009) 3230.
- [13] M. Rooth, R.A. Quinlan, E. Widenvist, J. Lu, H. Grennberg, B.C. Holloway, A. Härsta, U. Jansson, J. Cryst. Growth 311 (2009) 373.
- [14] Q. Fan, B. McQuillin, A.K. Ray, M.L. Turner, A.B. Seddon, J. Phys. D Appl. Phys. 33 (2000) 2683.
- [15] H. Iwasaki, K. Sudoh, Jpn. J. Appl. Phys. 41 (2002) 7496.
- [16] F. Zhang, Y. Zhang, S. Song, H. Zhang, J. Power Sources 196 (2011) 8618.
- [17] M. Pfanzelt, P. Kubiak, M. Fleischhammer, M. Wohlfahr-Mehrens, J. Power Sources 196 (2011) 6815.
- [18] M. Pfanzelt, P. Kubiak, S. Jacke, L. Dimesso, W. Jaegermann, M. Wohlfahr-Mehrens, J. Electrochem. Soc. 159 (2012) A809.
- [19] M.D. Levi, D. Aurbach, J. Phys. Chem. B 101 (1997) 4630.